Chem Biol Drug Des 2010; **76:** 100–106

doi: 10.1111/j.1747-0285.2010.00991.x

Research Article

Design of Potent IGF1-R Inhibitors Related to Bis-azaindoles

Conception Nemecek[1], William A. Metz[2], Sylvie Wentzler[1], Fa-Xiang Ding[2], Corinne Venot[3], Catherine Souaille[4], Anne Dagallier[4], Sébastien Maignan[4], Jean-Pierre Guilloteau[4], François Bernard[1], Alain Henry[1], Sandrine Grapinet[1] and Dominique Lesuisse[5,*]

[1]Medicinal Chemistry, Sanofi-aventis, 13 Quai Jules Guesde, 94300 Vitry-sur-Seine, France
[2]Medicinal Chemistry, Sanofi-aventis, Route 202-206, Bridgewater, NJ 08807, USA
[3]Oncology Department, Sanofi-aventis, 13 Quai Jules Guesde, 94300 Vitry-sur-Seine, France
[4]Structural Biology and Drug Design, Sanofi-aventis, 13 Quai Jules Guesde, 94300 Vitry-sur-Seine, France
[5]Sanofi-aventis, 1 av Pierre Brossolette, 91385 Chilly-Mazarin, France
**Corresponding author: Dominique Lesuisse, dominique.lesuisse@sanofi-aventis.com*

From an azaindole lead, identified in high throughput screen, a series of potent bis-azaindole inhibitors of IGF1-R have been synthesized using rational drug design and SAR based on a *in silico* binding mode hypothesis. Although the resulting compounds produced the expected improved potency, the model was not validated by the co-crystallization experiments with IGF1-R.

Key words: drug discovery, enzyme structure, kinase, phosphatase, structure-based drug design

Received 5 February 2010, revised 10 April 2010 and accepted for publication 18 April 2010

Insulin-like growth factor (IGF) promotes growth and mediates metabolic signals (1). There is evidence that links IGF to cancer or tumorigenesis, and examination of the literature (2–5) from the last decade suggests that agents capable of inhibiting IGF receptor would have potential in the treatment of such malignancies (6). To date, the first results from clinical trials on antibodies or small molecules targeting IGF-1 receptor are starting to be reported and confirm these hypotheses (7). We now wish to report our own findings in this area.

We initiated a high throughput screen (HTS) on IGF1-R using an Homogeneous Time-resolved Fluorescence (HTRF) assay relying on the receptor autophosphorylation. This led to the identification of a very potent hit **1** belonging to an azaindole chemical series from a Syk kinase inhibitor program (8).

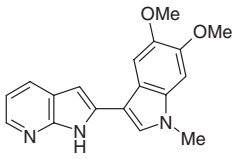

1

IC_{50} = 55 nM

As **1** was already quite potent on the target, we decided to evaluate it in an extensive panel of biological, Absorption, Distribution, Metabolism, Elimination (ADME), drug metabolism and Pharmacokinetics assays to anticipate potential liabilities and set the objectives of our optimization program.

We first evaluated **1** in a series of secondary assays related to IGF function. The potency in an ELISA IGF1-R autophosphorylation assay was comparable to the one obtained in the HTRF assay. Compound **1** was also able to inhibit the IGF1-induced proliferation in two different cell lines, a Mouse Embryonic Fibroblasts (MEF) cell line engineered to over express IGF1-R and an MCF7 breast tumor cell line, with IC_{50} 's of 1.6 and 4.3 μM, respectively (Table 1).

Selectivity against a panel of kinases was also evaluated. As expected because of its origin, **1** was a potent Syk inhibitor (Table 2). As expected also because of its high homology, there was no selectivity versus insulin receptor kinase (IRK). Inhibitors of IRK would be expected to induce insulin resistance (hyperglycemia). It was hypothesized that for a short treatment period (about 4 months), there should not be any major metabolic disturbances (compared with the physiological insulin resistance during late state of pregnancy). In addition, some dual inhibitors of IGF1-R and IR-A such as 1H-Benzoimidazol-2-yl)-1H-pyridin-2-one BMS-536924 (9) are undergoing preclinical studies and could be advantageous for the treatment of tumours expressing both IGF1-R and IR-A (10). Finally, some inhibitors in development, such as the pyrrolo[2,3-d]pyrimidine NVP-AEW541 (11) displayed good selectivity for IGF1-R versus IR in intact cells in spite of no enzymatic selectivity for the kinases. Owing to the little experience at that time with non-selective IGF-R inhibitors, it was decided to assess the possible drawbacks of an unselective inhibitor later in the development. From this initial kinase panel, only KDR and GSK3β were inhibited albeit at higher concentrations (3.6 and 5.5 μM, respectively).

Solubility, transport, and human metabolism of **1** were acceptable, and there was no PGP efflux. A preliminary single PK in rat showed

Table 1: Evaluation of **1** in IGF1-related assays[a]

	IGF1-R (HTRF) (μM)	IGF1-R (ELISA) (μM)	IGF1-induced proliferation (MEF) (μM)	IGF1-induced proliferation (MCF7) (μM)
1	0.055	0.145	1.6	4.3

[a]Briefly, the activities were determined as follows: *IGF1R–HTRF*: Inhibition of autophosphorylation activity was determined using a time-resolved fluorescent assay. The cytoplasmic domain of human IGF1R has been cloned as glutathione S-transferase (GST) fusion into the pFastBac–GST-tagged baculovirus expression vector. The protein has been expressed in SF21 cells and purified to about 80% homogeneity. Kinase activity was determined in 50 mM Hepes pH 7.5 containing 5 mM MnCl2, 50 mM NaCl, 3% Glycerol, 0.025% Tween 20, 120 μM adenosine triphosphate. Enzyme reactions were terminated by the addition of 100 mM Hepes buffer pH 7.0, containing 0.4 M KF, 133 mM EDTA, BSA 0.1% containing an anti-GST antibody labeled with XL665, and an anti-phosphotyrosine antibody conjugated to a europium cryptate (Eu-K). Features of the two fluorophores, XL-665 and Eu-K, are given in G.Mathis *et al.*, Anticancer Research, 1997, 17, pages 3011-3014. The specific long time signal of XL-665, produced only when the IGF1R enzyme is autophosphorylated, was measured on a Victor analyser (Perkin-elmer Life and Analytical Sciences, Courtaboeuf, France). Inhibition of IGF1R kinase activity with compounds of the invention was expressed as percentage inhibition of control activity exhibited in the absence of test compounds.
IGF1R–ELISA: Inhibition of autophosphorylation in MCF7 cell line after IGF1 stimulation was evaluated by ELISA technique. MCF-7 cells were seeded at 600 000 cells per well in 6-multiwell plates, left over night in 10% serum and then serum-starved for 24 h. Compounds are added to medium 1 h before IGF1 stimulation. After 10 min of IGF1 stimulation, cells are lysed with Hepes 50 mM pH7.6, Triton X100 1%, Orthovanadate 2 mM, proteases inhibitors. Cell lysates are incubated on 96-multiwell plates precoated with anti-IGF1R antibody, followed by incubation with an anti-phosphotyrosine antibody coupled to peroxidase enzyme. Peroxidase activity level (measured by OD with a luminescent substrate) reflects receptor phosphorylation status.
IGF1-Induced MCF7 cell proliferation: The antiproliferative effect of the molecules on MCF-7 cells was evaluated by [^{14}C]-thymidine uptake 72 h after IGF1-induced cell proliferation. MCF-7 cells were seeded at 25 000 cells per well in Cytostar 96-multiwell plates (Amersham Saclay, France) at 37 °C, 5% CO_2, at day 1, left overnight in EMEM medium supplemented with 10% of FCS to allowed cell attachment. At day 2, the medium culture was changed for EMEM/HamF12, 50/50 in order to deprive the cells for 24 h. On day 3, cell medium was replaced by fresh EMEM with 1 % of sodium pyruvate, penicillin, streptomycin, and 50 ng/mL final concentration of IGF1. Then, 0.1 μCi of [^{14}C]-Thymidine and 3 μL of compounds were added in 213 μL final volume. Cells were incubated at 37 °C, 5% CO_2 for 72 h. [^{14}C]-Thymidine uptake was quantified by counting the radioactivity 72 h after IGF1-induced proliferation (Microbeta trilux counter, Perkin-elmer). IC_{50} determination was performed in duplicate with 10 increasing concentrations.

Table 2: Evaluation of **1** in a panel of kinases

Kinase	IC_{50} (μM)	ATP (μM)[a]	Kinase	IC_{50} (μM)	ATP (μM)
SYK	0.055	2	PLK1	>10	40
IRK	0.086	250[b]	bARK	>10	6
IGF1-R	0.055	120[c]	CK1	>10	40
	0.280	40			
AURORA2	>10	40	Tie2	>10	20
KDR	>10	20	Rock2	>10	40
GSK3b	5.480	16	PKCd	>10	30
FAK	>10	1	CK2	>10	8
AKT	>10	80	Cdk2	>10	30
CDK4	>10	30	Src	>10	160
JNK3	>10	6	PKA	>10	20
P38	>10	300	PDK4	>10	32
PAK3	>10	1.7	MEKK1	>10	20

IRK, insulin receptor kinase
[a]Internal kinase profiling; [ATP] = 2 Km.
[b]Coupled PK-LDH assay.
[c]HTRF assay.

acceptable exposure and bioavailability in spite of a high clearance and short half-life (Table 3). Cytochrome P450 (CYP) inhibition did not appear to be an issue (human recombinant CYP 3A4, 1A2, 2D6, 3C9, 2C19 enzymes, data not shown).

The goals of our optimization program were therefore set by this initial analysis: optimize potency, in particular cellular potency and selectivity versus Syk and other closely related kinases and optimize metabolic stability to achieve a half-life of around 5 h in mice. This article deals with optimization of the potency.

Even though we had no experimental information on the binding mode of **1** in IGF1-R, the SAR data we had supported the hypothesis that the two nitrogen atoms N1 and N7 of the azaindole moiety were interacting with the hinge portion of the kinase (12). Indeed, removing N7 in the bis-indole **2** resulted in total loss of the IGF1-R inhibiting activity. On the other hand, moving this nitrogen atom around the aromatic ring from position 7 to position 4 of the azaindole (data not shown) also led to loss of activity. The fact that methylation on the N1-position of the azaindole showed complete loss of activity, further strengthened this binding hypothesis.

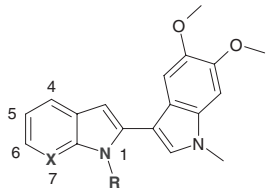

1 X = N R = H 55 nM
2 X = C R = H > 10 μM
3 X = N R = Me >10 μM

Even though this hit arose from a series that had already been thoroughly investigated in the Syk program, we could gather relatively little information about the SAR for IGF1-R because the 5′-methoxy group was essential to the activity. Table 4 shows the subsequent loss of activity with removal of the methoxy groups on the indole ring. We therefore designed a program of chemical modifications keeping these groups in place.

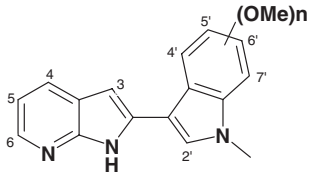

Substitution on positions 3 and 2′ on the azaindole and indole respectively also proved to be detrimental to the activity. On the

Table 3: Solubility, ADME and PK profile of **1**

Sol (mg/mL)						*In vivo* PK[d]			
pH 7.4	pH 2.7	Met Stab[a,b]	Met Stab[a,c]	$CaCo_2$ P total	Efflux ratio	AUC po (h μg/mL)	F[e] (%)	Cl[f] (L h/kg)	t1/2 po (h)
0.010	24.4	70	26	156	1.36	5.32	52	4.9	1.5

[a]Percent of compound remaining after 15 min of S9 fraction exposure.
[b]Human S9 hepatic fraction.
[c]Mouse S9 hepatic fraction.
[d]Rat; Vehicle 5%PS80. 4%HCl 0.1 N in Gluco5%; 50 mpk.
[e]Bioavailability.
[f]Clearance.

Table 4: Activity as a function of methoxy position

Cpd	Position of MeO	IGF1-R (HTRF) (μM)
1	5′, 6′	0.055
4 (8)	5′	0.65
5	5′, 7′	1.6
6	6′	>10
7	4′, 5′	>10

other hand, the 6′-position was more permissive as was also the case for the 1′-position. These positions were heavily explored with production of libraries of various alkoxy, alkyl, and alkyl-substituted side chains, but even if some derivatives were able to, at best, keep the activity of the starting prototype, no substantial gain of affinity was seen (data not shown) and we kept some of these in mind for final modulation of the physicochemical properties like solubility (see later).

Position 4, 5, and 6 on the azaindole were substituted with halogens and a few other groups (Table 5) showing that small hydrophobic substituents on position 4 like chlorine (**8**), nitrile (**9**), and alkyls (**10** and **12**) are well tolerated (IC_{50}'s 43–168 nM) while polar substituents like amine (**14**, IC_{50} 3 μM) and larger substituents resulted, most of the time, in loss of affinity. Position 5 only accepted limited changes with fluorine (**11**) even displaying activity enhancement (IC_{50} 19 nM) while activity dropped rapidly with chlorine (**13**) displaying an IC_{50} of 400 nM. Disappointingly, the introduction of a primary amine in position 6 as in **16**, to improve the affinity by adding a hydrogen bond with the hinge, resulted in loss of activity.

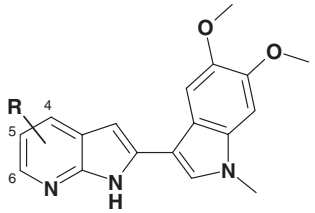

The crystallization of IGF1-R is complicated by the fact that the receptor exists under various stable conformations depending on its phosphorylation state. At the time we initiated this work, X-Ray data were publicly available for the 0- (13), 2- (14), and 3- (15)

Table 5: Activity as a function of methoxy position

Cpd	R and position	IGF1-R (HTRF) (μM)
8	4-Cl	0.043
9	4-CN	0.062
10	4-Me	0.104
11	5-F	0.019
12	4-CH_2OH	0.168
13	5-Cl	0.406
14	4-NH_2	3
15	6-Cl	>10
16	6-NH_2	>10

phosphorylated forms but we had no in-house experimental co-structure of an azaindole with IGF1-R. A 3D homology model was built using the ATP-bound structure of a 3-phosphorylated form of IGF1-R (PDB code 1K3A). Figure 1A shows a ribbon representation of the ATP-binding site, highlighting the hinge portion which contains the hydrogen bond partners of ATP and the solvent region. In terms of structure-based drug design, our knowledge of this chemical series was enriched by experimental 3D structures solved in-house of various azaindole analogs complexed with Jnk3 and Aurora2 kinase domains. The position of the azaindole scaffold is the same, in all structures, with the azaindole nitrogen atoms hydrogen-bonded to the hinge backbone and the indole substituent lying along the backbone at the entry of the ATP-binding site. Docking calculations allowed proposing two binding modes. The first one, showed in Figure 1B, is similar to the one observed in Jnk3 and Aurora2. The second one places also the indazole moiety in front of the hinge region, but the indole ring is flipped 180° around the C-C bond between the two bicycles, as shown in Figure 1C. This ligand conformation is allowed in IGF1-R because of a small hydrophobic pocket which can accommodate the 5′-methoxy group, with a Leucine residue in the hinge region (Leu1051), where a Tyrosine and a Leucine residue are found in Aurora2 and Jnk3, respectively. Our SAR data in particular in position 5′ along with the selectivity of the compounds versus Aurora2 and Jnk3 supported the hypothesis of the alternative binding mode.

To assess this binding hypothesis, we introduced a nitrogen atom on position 4′ of the indole to stabilize this conformation through an internal hydrogen bond and increase the inhibitory activity of the compound. Quantum mechanics calculations favour this form by

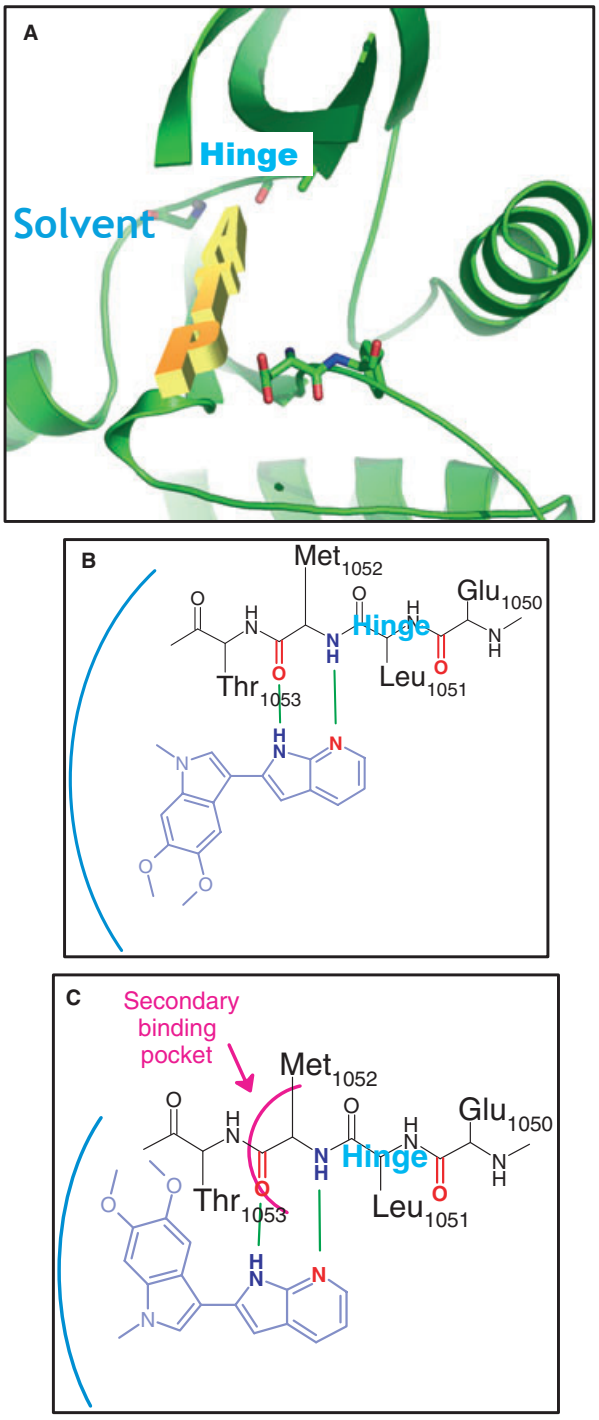

Figure 1: (A) Ribbon representation of a schematic kinase ATP-binding site; (B) azaindazole-binding mode in IGF1-R similar to Jnk3 and Aurora2; (C) alternative binding mode in IGF1-R (same orientation of ATP site in all figures).

3–4 kcal/mol,[1] a value compatible with a hydrogen bond. Indeed, the addition of this nitrogen as in **17** resulted in substantial activity improvement with an IC_{50} of 6 nM for IGF1-R inhibition.

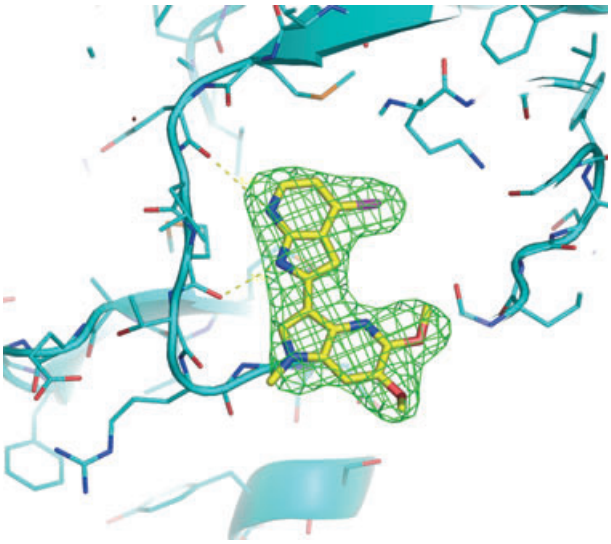

Figure 2: X-Ray of **25** with IGF1-R 2P form (resolution 3 Å).

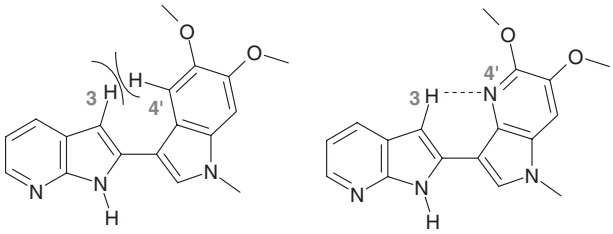

Figure 3: Active conformations of **1** (left) and **17** (right) bound to IGF1-R.

Table 6: Activity as a function of azaindole substitution

Cpd	X	R'1	R4	R5	IGF1-R (HTRF) (nM)	IGF1-induced proliferation (MEF) (nM)
1	C	Me	H	H	54	1600
18	C	CH_2CH_2Morpholine	H	H	58	1100
8	C	Me	Cl	H	43	305
19	C	CH_2CH_2Morpholine	Cl	H	27	749
20	C	CH_2CH_2PiperazineNMe	Cl	H	15	301
11	C	Me	H	F	19	117
21	C	CH_2CH_2Morpholine	H	F	22	215
22	C	CH_2CH_2PiperazineNMe	H	F	23	169
23	C	CH_2CH_2Morpholine	Cl	F	5.5	26
17	N	Me	H	H	6.4	198
24	N	CH_2CH_2Morpholine	H	H	4.8	11
25	N	Me	Cl	H	2	184
26	N	CH_2CH_2Morpholine	Cl	H	1.5	1.1
27	N	CH_2CH_2Morpholine	H	F	2.6	8
28	N	CH_2CH_2Morpholine	Cl	F	22	32

Table 7: Activity of **26** on a panel of cell lines

Tissue	Cell line	IC_{50} (μM)
NSCLC[a]	A549	1.49
NSCLC[a]	H460	1.49
NSCLC[a]	H1299	1.18
Colon	HCT116	3.1
Colon	HT29	0.14
Uterus	HeLa	2.12
Prostate	PC3	7.1
Prostate	DU145	6.44

[a]Non-small cell lung cancer.

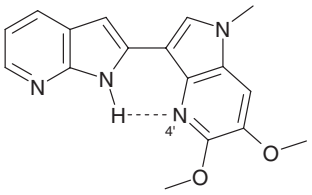

17 (6 nM)

We finally succeeded in obtaining crystal structures of IGF1-R complexed to azaindazole analogs. Compound **25** was co-crystallized with the bisphosphorylated form of IGF1-R[2] demonstrating that the bound conformation is the same as the one observed in Aurora2 and Jnk3, displayed in Figure 1B (Figure 2). Subsequent crystallographic structures with azaindole analogs complexed to IGF1-R showed the same binding conformation (data not shown).

Thus quantum mechanics energy calculations on the unbound **17** did not explain the observed improvement of activity. A hypothesis for the observed activity enhancement of the bis-azaindole series is that the presence of the 4′-nitrogen atom favors the active flat conformation of the two bicycles observed in the crystallographic structure by removing the steric clash between the 3- and 4′-hydrogens in **1**. There might even be a small additional stabilization through an internal hydrogen-bond between 4′-N and azaindole 1-H atoms even though this type of H-bond is not very documented in the literature (Figure 3).

We kept this new bis-azaindole scaffold in our final optimization. The best compounds resulting from our chemistry effort are summarized in Table 6. Overall, the 10-fold activity enhancement was observed for all compounds with a nitrogen atom at position 4′ of the indole moiety (**17** and **24**–**28**) compared to equivalent analogs with a carbon atom (**1**,**8**,**11**,**19**–**23**). This modification has also resulted in a striking impact on the cellular activity, the most potent compound (**26**) displaying a potency of 1 nM in the MEF IGF-induced proliferation assay. Also, quite interesting was the effect of the aminoethyl side chains at position 1′ of the azaindole on the cellular potency (compare for instance **17** with **24** and **25** with **26**). This effect was much less pronounced on the initial carbon

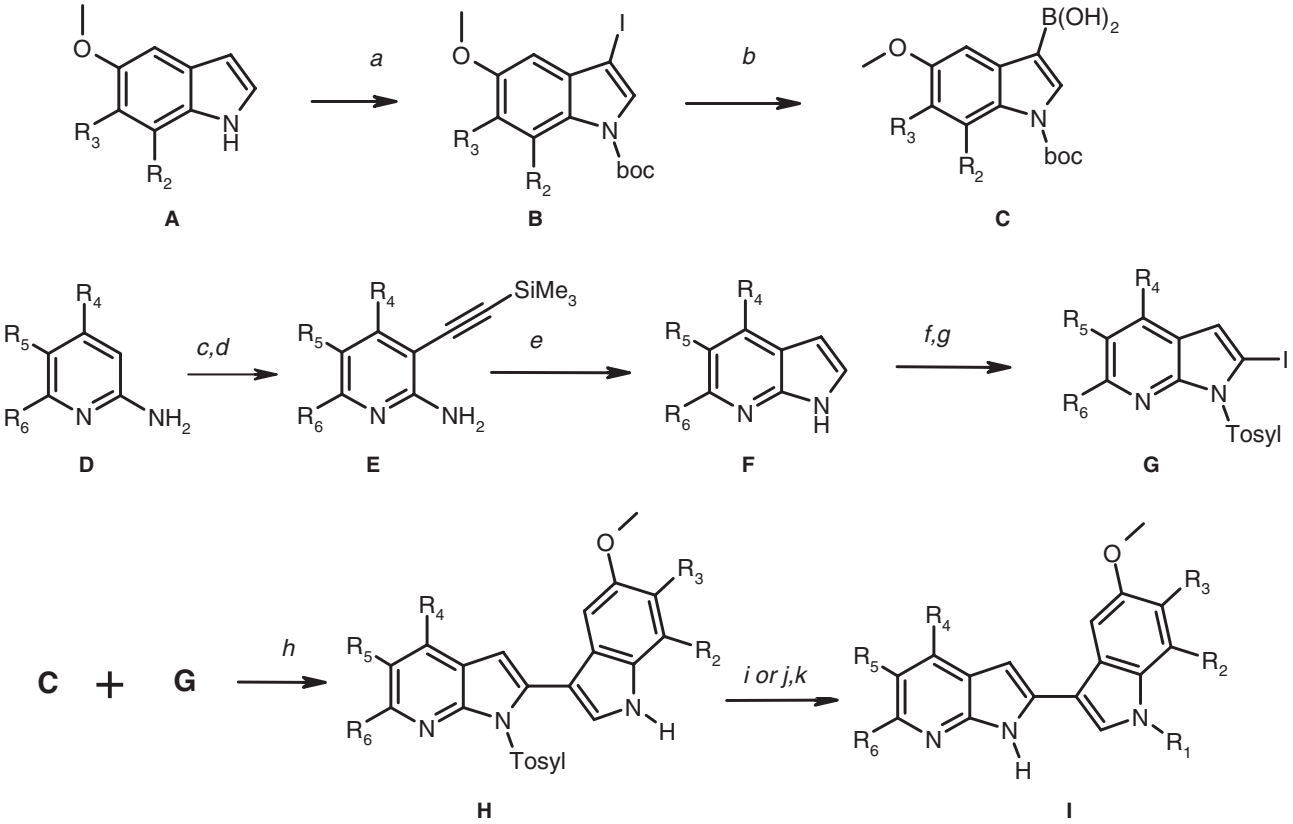

Scheme 1: Reagents and conditions : a. KOH, I_2, DMAP, MeI, DMF or KOH, I_2, DMAP, $(Boc)_2O$, DMF; b. nBuLi, $B(OMe)_3$; c. NIS,AcOH; d. TMS-Ethynyl, CuI, LiCl, TEA, $PdCl_2$(dppf), DMF; e. t-BuOK, NMP, 70 °C; f. TsCl, BuN_4NHSO_4, NaOH, H_2O, toluene; g. BuLi, THF, I_2; h. $Pd(PPh_3)_4$, $NaHCO_3$ aq, DMF, 110 °C; i. NaH, DMF, MeI; j. K_2CO_3, DMF, $ClCH_2CH_2$morpholino/HCl; k. KOH, MeOH reflux.

series. Compound **26** proved a tight binding IGF1-R inhibitor with a Ki of 1.6 nM (data not shown). It was kept for further profiling.

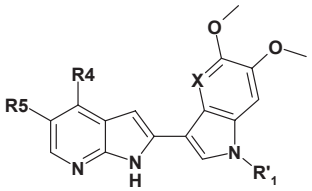

Compound **26** was profiled in a panel of proliferating cell lines. The huge improvement of potency in the MEF cell line did not translate into the same improvement versus these additional cell lines. The best responding cell line turned out to be HT29, a colon cell line, with an IC_{50} of 140 nM (Table 7).

The general synthesis of the 2-(3-indolyl)-7-azaindoles **4, 5, 8 11, 13, and 18–22** (compounds **I**) is outlined in Scheme 1 (16). The substituted 1-Boc-3-boronic acids 5-methoxy-indoles **C** were obtained from 5-methoxyindole **A** after iodination in position 3 under basic conditions followed by iodine lithium exchange and trapping with trimethylborate. The substituted 7-azaindoles **F** were synthesized from the corresponding 2-aminopyridines **D** after 3-iodination, displacement of the 3-iodine by a trimethylsilylethynyl (17,18) group, and cyclization under basic conditions. The resulting azaindoles **F** were protected on the nitrogen by a tosyl group and iodinated under basic conditions to afford the 2-iodo derivatives **G**. These two building blocks **C** and **G** underwent palladium-catalyzed coupling to afford the bis-bicyclic derivatives **H**. Alkylation on the indole under basic conditions followed by deprotection of the tosyl group afforded the final compounds **I**. From these, functional modifications led to the azaindoles **9**, **10, 12,** and **14**[1].

The general synthesis of the 2-[3-(4-azaindolyl)]-7-azaindoles **17**, **24**–**28** (compounds **R**) is outlined in Scheme 2 (19). The 4-azaindole-building block **N** was obtained via a quite original synthesis: the 3-hydroxy-2-bromo-pyridine **J** was converted to the 2,3-dimethoxy-6-iodo-pyridine **K** after iodination (20) in position 6 followed by methylation of the phenol and substitution of the 2-bromine by sodium methoxide. Metal lithium exchange with nBuLi followed by formylation with Dimethylformamide (DMF) afforded the 6-formyl derivative which was nitrated at position 5 with cupric nitrate trihydrate (21). Condensation with nitro methane under classic Henry conditions (22,23) followed by a modified procedure reported by Novellino (24) gave the hydroxylated nitrostyrene which upon heating with sodium acetate in acetic anhydride gave the nitrostyrene intermediate **L** as a mixture of isomers. Silica gel-assisted reductive cyclization (25) of this unstable intermediate,

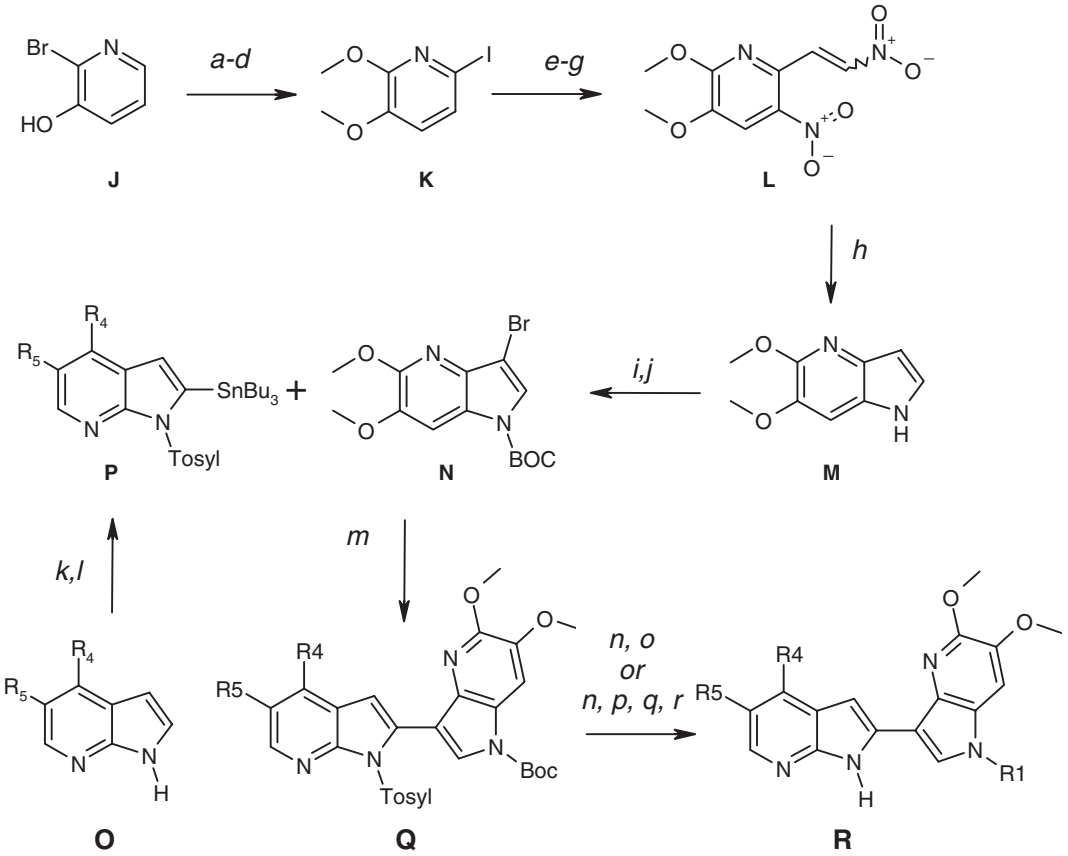

Scheme 2: Reagents and conditions : a. K_2CO_3, I_2, H_2O; b. MeI, K_2CO_3, DMF; c.NaOMe, DMF, 100 °C; d. nBuLi,/THF, −78 °C, DMF; e. Ac_2O,$Cu(NO_3)_2{\cdot}3H_2O$,; f. NaOEt, $MeNO_2$,THF/EtOH, HCl.; g. NaOAc, Ac_2O, reflux; h. Fe, SiO_2, AcOH, tol.uene, reflux; i. Br_2,, DMF, −15 °C; j. Boc_2O, DMAP, TEA, DMF; k. $ClSO_2Ph$-Me, NaOH, $(nBu_4)NHSO_4$; l. nBuLi, $(nBu_3)SnCl$, THF, −75 °C; m. $Pd(PPh_3)_4$, CuI, toluene, reflux; n. TFA, AcOH, CH_2Cl_2; o. NaH, DMF, MeI; p. $Cl(CH_2)_2Cl$, Bu_4NBr, KOH, Na_2CO_3, 50 °C; q. NaI, MEC; r. morpholine, K_2CO_3, CH_3CN, reflux.

with iron in acetic acid, provided the desired 4-azaindole **M**. This compound was further brominated in position 3 and protected with Boc-carbonate to afford **N**. On the other hand, the 7-azaindoles **O** were protected with a tosyl group which then allowed the specific introduction of the tributyltin moiety in position 2 to afford **P**. Compounds **P** and **N** were coupled using standard Stille conditions and after subsequent deprotection of the Boc and tosyl groups, followed by N-alkylations the desired compounds **R** (cpds **17**, **24**–**28**) were obtained (Scheme 2).

A lead from HTS was optimized for the inhibition of IGF1-R using rational drug design. This led to the discovery of a very potent series of bis-azaindoles, although the subsequent crystallographic experimental data did not confirm the binding mode proposed by the *in silico* calculations.

Acknowledgments

We are grateful to Antonio Guerreiro and Catherine Souaille for helpful discussions and to the analytical department for compound analyses.

References

1. Kim J.J., Accili D., Naomi B. (2002) Signalling through IGF-I and insulin receptors: where is the specificity? Growth Horm IGF Res;12:84.
2. Furstenberger G., Senn H.-J. (2002) Insulin-like growth factors and cancer. Lancet Oncol;3:298.
3. Gross J.M., Yee D. (2003) The type-1 insulin-like growth factor receptor tyrosine kinase and breast cancer: Biology and therapeutic relevance. Cancer Metastasis Rev;22:327.
4. Yu H., Rohan T. (2000) Role of the insulin-like growth factor family in cancer development and progression. J Natl Cancer Inst;92:1472.
5. Bohula E.A., Playford M.P., Macaulay V.M. (2003) Targeting the type 1 insulin-like growth factor receptor as anti-cancer treatment. Anticancer Drugs;14:669.
6. Zhang H., Yee D. (2004) The therapeutic potential of agents targeting the type I insulin-like growth factor receptor. Expert Opin Investig Drugs;13:1569.
7. Gualberto A., Pollak M. (2009) Emerging role of insulin-like growth factor receptor inhibitors in oncology: early clinical trial results and future directions. Oncogene;28:3009.
8. Cox P.J., Majid T.N., Lai J.Y.Q., Morley A.D., Amendola S., Deprets S., Edlin C. (2001) Preparation of azaindoles as protein kinase inhibitors. PCT Int Appl 270 WO 03/000688 A1.
9. Wittman M., Carboni J., Attar R., Balasubramanian B., Balimane P., Brassil P., Beaulieu F. *et al.* (2005) Discovery of a 1H-Benzoimidazol-2-yl-1H-pyridin-2-one (BMS-536924) Inhibitor of Insulin-like Growth Factor I Receptor Kinase with in Vivo Antitumor Activity. J Med Chem;48:5639.
10. Yuen J.S.P., Macaulay V.M. (2008) Targeting the type 1 insulin-like growth factor receptor as a treatment for cancer. Expert Opin Ther Targets;12:589.
11. Garcıa-Echeverrıa C., Pearson M.A., Marti A., Meyer T., Mestan J., Zimmermann J., Gao J. *et al.* (2004) In vivo antitumor activity of NVP-AEW541 as a novel, potent, and selective inhibitor of the IGF-IR kinase. Cancer Cell;5:231.
12. Ghose A.K., Herbertz T., Pippin D.A., Salvino J.M., Mallamo J.P. (2008) Knowledge Based Prediction of Ligand Binding Modes and Rational Inhibitor Design for Kinase Drug Discovery. J Med Chem;51:5149.
13. Munshi S., Kornienko M., Hall D.L., Reid J.C., Waxman L., Stirdivant S.M., Darke P.L., Kuo L.C (2002) Crystal structure of the apo, unactivated insulin-like growth factor-1 receptor kinase. Implication for inhibitor specificity. J Biol Chem;277:38797.
14. Pautsch A., Zoephel A., Ahorn H., Spevak W., Hauptmann R., Nar H. (2001) Crystal structure of bisphosphorylated IGF-1 receptor kinase. Insight into domain movements upon kinase activation. Structure (Cambridge, MA, United States);9:955.
15. Favelyukis S., Till J.H., Hubbard S.R., Miller W.T. (2001) Structure and autoregulation of the insulin-like growth factor 1 receptor kinase. Nat Struct Biol;8:1058.
16. Wentzler S., El Ahmad Y., Filoche Romme B., Nemecek C., Venot C. (2005) Fr. Demande 217 pp.; WO2006/037875.
17. Kumar V., Dority J.A., Bacon E.R., Singh B., Lesher G.Y. (1992) Synthesis of 7-azaindole and 7-azaoxindole derivatives through a palladium-catalyzed cross-coupling reaction. J Org Chem;57: 6997.
18. Koradin C., Dohle W., Rodriguez A.L., Schmid B., Knochel P. (2003) Synthesis of polyfunctional indoles and related heterocycles mediated by cesium and potassium bases. Tetrahedron;59:1571.
19. Nemecek C., Metz W., Wentzler S., Lesuisse D. (2006) Fr. Demande 110 pp. WO2005/095399.
20. O'Neill B.T., Yohannes D., Bundesmann M.W., Arnold E.P. (2000) Total synthesis of (+/-)-cytisine. Org Lett;2:4201.
21. Sinhababu A.K., Borchardt R.T. (1988) Independent synthesis of 5-hydroxytryptamine-4,7-dione, the neurocytotoxic product of autoxidation of 5,7-dihydroxytryptamine. J Heterocycl Chem;1988:25.
22. Rosini G., Ballini R., Sorrenti P. (1983) Synthesis of 2-nitroalkanols on alumina surfaces without solvent: a simple, mild and convenient method. . Synthesis;6:1014–1016.
23. Henry L. (1895) Formation. synthétique d'alcools nitrés. C R Acad Sci Paris;120:1265.
24. Novellino L., d'Ischia M., Prota G. (1999) Expedient Synthesis of 5,6-Dihydroxyindole and Derivatives via an Improved Zn(II)-Assisted 2,b-Dinitrostyrene Approach. Synthesis;5:793–796.
25. Sinhababu A.K., Borchardt R.T. (1983) Silica gel-assisted reduction of nitrostyrenes to 2-aryl-2-[2H]-1-nitroethanes with sodium borodeuteride. J Org Chem;48:3347.

Notes

[1]Systematic conformational analysis with the Merck molecular force field. (Thomas A. Halgren, I. Basis, form, scope, parameterization, and performance of MMFF94, J. Comp. Chem.; 1996; 490–519) then geometry optimisation using Density Functional Theory (B3LYP/6-31G*), no statistical thermodynamics corrections were applied. Calculation done with Spartan08 (Wavefunction).

[2]Crystal structure of **25** with IGF1-R have been deposited in the PDB with accession code 3LVP.